Modern Approaches to the Applying of Mathematical Methods in the Analysis of the Transport Direction of Follicular Thyrocytes

Olha Ryabukha[a], and Ivanna Dronyuk[b]

[a] *Lviv Medical Institute, Polishchuk str. 76, Lviv, 79018, Ukraine*
[b] *Lviv Polytechnic National University, S. Bandera str. 12, Lviv, 79013, Ukraine*

Abstract

The use of modern information technology in biomedical research permits to obtain a holistic cybernetic view of the cell. The method of constructing correlation portraits of different fields of hormone-producing cells' activity has significantly expanded the approaches to studying the relationships between their ultrastructures in different conditions. However, the significance of the portrait nodal points for cell activity remains unclear. This paper first presents a step-by-step study of the nodal points of correlation portraits of follicular thyrocytes' transport capability, which consists in elucidating their connection filling, the studied correlations between their constituent elements, analyzing the effect of the established transport features of hormonal product by intraorganic microcapillary bed under the effect of organic and inorganic iodine. It is established that the nodal points of correlation portraits are mathematical results of stabilizing and adapting changes in hormonal cells, the study of which will permit to better understand the functional dependencies that occur in the cell during its activity.

Keywords 1

mathematical methods in cytology, correlation analysis, correlation portrait, thyroid gland, follicular thyrocyte, thyroid hormone transport, organic iodine, inorganic iodine, iodine deficiency

1. Introduction

This work is a continuation of a series of our studies prioritized in this field of science, previously presented at IDDM'2018 [1] and IDDM'2020 [2].

We base our concept of cytological research on the approach to the cell as a cybernetic self-regulatory system. Based on these ideas, the animal cell is subject to many different external and internal influences, with internal influences being divided into influences of other cells of the same organ and influences of different body systems cells. The point of application of influences in the cell are cellular ultrastructures, which are strictly functionally specialized and implement a specific field of the cell activity [3]. At the same time, the same field of cell activity is usually implemented by several ultrastructures that form a respective cluster. In this case, influences of different nature and force can act on different constituent elements (ultrastructures or their substructures) of the same cluster. The effect of influences is due to the transformation of cell activity depending on the type of influence, its strength and functional ability of the target organelle and the cell as an integrating structure. Then it is logical to assume that the resulting effect of different factors' influences that have the same field of action but are directed to different ultrastructures of the same cluster, may have some differences.

IDDM-2021: 4th International Conference on Informatics & Data-Driven Medicine, November 19–21, 2021 Valencia, Spain
EMAIL: oriabuha@ukr.net (Olha Ryabukha); ivanna.m.droniuk@lpnu.ua (Ivanna Dronyuk)
ORCID: 0000-0001-6220-4381 (Olha Ryabukha); 0000-0003-1667-2584 (Ivanna Dronyuk)

One of the prerequisites for the functioning of the biological system is its diversity – the number of states that it can acquire under certain conditions [4]. Diversity does not only determine the complexity degree of the biosystem organization [5], but can also indicate its adaptive potential. In addition, all biological systems have a high level of adaptability, which permits them not only to survive in the changing conditions of existence, but also to function in new conditions. Since each system has certain reserves, the prerequisites are created to determine the characteristics of the biological system both in a state of functional equilibrium and to identify its potential [6].

The task of biomedical diagnostics is to establish the dependence of the diagnosis on many state parameters of the studied system. Then the task of medical diagnosis is to find a expression

$$X^* = (x_1^*, x_2^*, x_3^*, \dots, x_n^*) \to d_j \in D = (d_1, d_2, d_3, \dots, d_m)\,, \quad (1)$$

where X^* is a set of a particular patient's state parameters, and D is a set of diagnoses inherent in the given field of medicine.

However, the main mathematical methods used to solve diagnostic problems (Bayesian [7], regression [8], correlation analysis [9], etc.) are based on the use of quantitative information about a biological object, which limits their use in medicine-biological studies. It is quite promising to diagnose on the basis of fuzzy set theory [10], which permits to formalize the uncertainties that arise in the biological system and use Fuzzi Logic in the study of living bodies [11]. To do this, the concept of membership function is used and the largest and smallest expression of any feature (max-*y* and min-*y*), combined with the principle of linguistic diagnostic data [12]. The principle of linguistic diagnostic data presupposes the existence of causal relationships between the parameters of the biological system (cause) and the diagnosis (consequence), which are first described in words of the language used, and then formalized as a set of fuzzy logical statements. In this case, the formalization of the diagnostic process involves determining the diagnosis d through the input parameters (variables) x_1, x_2, x_3,…, x_n, which characterize the patient's condition. Then:

$$d = f_d(x_1, x_2, x_3, \dots, x_n)\,, \quad (2)$$

where f_d is some function that establishes a relationship between the variables x_i, $i = \overline{1,n}$ and d.

The variables $x_1 \div x_n$ and the function d can be quantitative, qualitative or expressed using special scales, for example, by a scoring system. This makes it possible to take into account the qualitative staining of the condition, which significantly expands the possibilities of establishing a correct diagnosis, but provides a strict determinism of the diagnosis on the input data, which is difficult to achieve when studying the cell.

Traditional methods of cytological examination are based on the use of either quantitative data about the object under study, or qualitative information that describes the state of this object. Quantitative definitions that can be subjected to mathematical transformation can not establish and analyze all the nuances of the cell's state as a biological system, while qualitative information about it, which is given in words of the language used and is able to note the slightest changes in its state under various influences, can not be calculated, and hence objectified. This does not permit to analyze, compare, summarize the data obtained and draw sound conclusions. Thus, approaches to the formalization of qualitative and binary information about the cell, despite its importance for medical science, remain undeveloped. In our previous publications, in particular [13], mathematical methods have been used to diagnose and interpret the effects of iodine of various chemical nature on thyroid cells. To do this, a package of certain mathematical methods was used, each being the basis for the next step [1]. Correlation portraits, which are a graphical representation of the traced correlations, are subject to analysis. The basis for their creation are "reference" points – ultrastructures, which are functionally significant for the implementation of the studied field of the cell's activity. Correlation portraits are constructed on the basis of "actual" features – ultrastructures of this field, between which significant correlations are traced. Comparison of nomenclatures of "reference" points and "actual" features and interpretation of the traced correlations values between cellular organelles from the standpoint of cytophysiology [14] permit both individualization and generalization of the obtained data as to the current state, reserve and potential hormone abilities in each field of its activity. At the same time, in the available literature we did not find information on the interpretation of the nodal points' connection filling in the study of follicular thyrocytes' ultrastructures in iodine intake of different chemical nature against the background of alimentary iodine deficiency, which is a very important medical and social problem [15].

2. Purpose of the study

The purpose of the presented work was to study the significance of the nodal points of correlation portraits as places that connect and unite the ultrastructures of the follicular thyrocytes' transport activity. The task of the study was to establish the value of nodal points for the transport of hormonal product by intraorgan microcapillary bed in the following model conditions: optimal supply of iodine to rats, uncorrected alimentary iodine deficiency, taking the minimum effective dose of organic and inorganic iodine.

3. Materials and methods of the study

The study was performed on 40 white nonlinear male rats with an initial body weight of 140–160g, which were kept in standard vivarium conditions for 30 days. Group 1 rats consuming common feed were universal controls for rats of other groups. Rats of groups 2, 3, 4 were on an isocaloric starch-casein diet; iodine-containing compounds were eliminated from the salt mixture to create a model of alimentary iodine deficiency. Adjustment of iodine starvation in rats of group 3 was performed with organic iodine (iodine-protein components), rats of group 4 – with inorganic iodine (potassium iodide), which they consumed in the minimum histologically confirmed dose of 21 μg/kg body weight. Iodine compounds were not added to the diet of group 2 rats, which were an additional control for animals of groups 3 and 4. During observation and euthanasia, the principles of bioethics were observed in compliance with the European Convention for the Protection of Vertebrate Animals Used in Experiments (Strasbourg, 1986) and Council of Europe Directive 2018/63/ CV.

The study methods used in this work have already been partially presented in detail by us at IDDM'2020 [2]: 1. *Mathematical statistics* [16]. 2. *The method of the phase interval* [17]. 3. *Correlation analysis* [18,19]. Correlations were established between the constituent elements of the profile of the follicular thyrocytes' transport capability and the pairwise correlation coefficients, which were calculated according to the well-known Pearson's formula, their direction and strength being studied. A positive value of the pairwise correlation coefficient r_{xy} indicated the same direction of changes of the studied index, negative – that with the increase of one of the indices associated with another index associated with it decreased: the value of r_{xy}= 1.00 indicates the existence of a directly proportional relationship between indices *x* and *y*, r_{xy}= –1.00 – inversely proportional. In the structural organization of the relationship between the indices, the most significant were considered to be very high and high connections, which according to the *Chaddock scale*, were within the range of $1.00 \geq r_{xy} \geq 0.91$ and $0.90 \geq r_{xy} \geq 0.71$, respectively; in the absence of such connections, salient connections of $0.70 \geq r_{xy} \geq 0.51$, and moderate connections of $0.50 \geq r_{xy} \geq 0.31$ were considered. 4. *Principles of fuzzy set theory* [10]. 5. *Method of Semi-Quantitative Analysis of Electronograms by Riabukha OI* [20]. Qualitative information about the cellular ultrastructures of the studied electron microscope images was transformed into quantitative by comparing their condition with the state of these ultrastructures in two controls (norm and untreated studied pathology) with subsequent assessment of the detected manifestations in points. The obtained numerical assessment results of each ultra- or substructure were to be averaged with further use for mathematical transformations. 6. *Method of Riabukha OI on Specifying the Profiles of Special Capabilities of Hormone Producing Cells* [20]. In our work, we present the ultrastructural components of the thyroid gland follicular thyrocytes' profile of the transport activity (Tab. 1).

7. *Construction of correlation portraits* [1]: Correlation portraits are a graphical representation of the relationships traced between the structural components of the studied transport activity of follicular thyrocytes. 8. *Study of correlation portraits' nodal points* as places for accumulation of correlations. There are five steps to learn about the nodal points. The first step is to construct correlation portraits of the studied possibility, the second – to determine the nodal points of each correlation portrait as graphical representations of correlations' clusters. The third step is to establish the connection content of each node, which is to determine the number and nomenclature of its correlations. In this case, the number and content of nodal points is not a constant value, but reflect the individual characteristics of the portrait. The fourth step is to rank the established nodal points on the main (points with the largest

filling of correlations) and additional (points with less correlation). The fifth step is to analyze the data obtained and establish from the standpoint of cytophysiology their significance for the activities of the studied activity.

Table 1
Ultrastructural components of the transport direction activity profile of the thyroid gland's follicular thyrocytes

Ultrastructural element	Studied feature of the ultrastructural element	Status of the studied ultrastructural element feature	Symbol legend of the studied ultrastructural element feature
Basal cytoplasmic membrane	folding	insignificant	P1
		moderate	P2
		significant	P3
Perycapillary space	width	insignificant	Q1
		moderate	Q2
		significant	Q3
	additional inclusions	present	Q4
		absent	Q5
Endotheliocytes	morpho-functional state	hypotrophic	R1
		unchanged (normal)	R2
		hypertrophic	R3
	pseudopodiae	small	R4
		medium (normal)	R5
		big	R6
Microcapillary bed	morpho-functional state	no features (normal)	S1
		stasis fenomena	S2
		presence of erythrocytes	S3
		thrombosis phenomena	S4
		presence of mast cells	S5
		presence of fibrin strands	S6

9. *Cytophysiological study*. The basis for the interpretation of correlation portraits' nodal points of the rat follicular thyrocytes' transport capability profile in the studied groups were cytophysiological data on the functional significance of cellular ultrastructures [3,14] and their electron microscopic characteristics. 10. *Electron microscopy*. Electronograms of ultrathin (4–6 μm) sections of rat thyroid glands, made according to generally accepted methods, were subject to study [21]. Processing of the obtained results was performed by the scale for assessment of thyrocyte ultrastructural elements' manifestations using the semi-quantitative analysis of electron microscope images by means of software: for digital data - StatSoft Statistica v6.0 package, for correlation tables and portraits - Microsoft Office 2010 package - electronic MS Excel spreadsheet and MS Word graphic editor (Microsoft Graph), respectively.

4. Results and discussion

Reference points for the construction of correlation portraits in all groups were moderate folding of the follicular thyrocytes' basal cytoplasmic membranes (P2), moderate width of the microvessels' pericapillary space (Q2), unchanged (normal) endotheliocytes (R2), no features (normal) microcapillary bed (S1). The main nodal points of correlation portraits were considered to be the points through which the most correlations pass, the additional nodal points are points with fewer correlations.

4.1. Studying the features of the nodal points of the transport capability profile correlation portrait of follicular thyrocytes of intact rats (group 1)

The actual features of the correlation portrait were P2, Q1, Q5, R2, R4, S1, between which the following correlations were observed: very high (1.00≥| r |≥ 0.91) – 2; high (0.90≥| r |≥ 0.71) – 0; salient (0.70≥| r |≥ 0.51) – 2; moderate (0.50≥| r |≥ 0.31) – 6 (all indirect). The main nodal points of the portrait were moderate folding of the basal cytoplasmic membranes of follicular thyrocytes (P2) and no features (normal) microcapillary bed (S1), which had 4 connections; additional nodal points of the portrait were an insignificant width of the pericapillary space (Q1), no additional inclusions in the pericapillary space (Q5), unchanged (normal) endotheliocytes (R2) and small pseudopodia of endotheliocytes (R4), which had 3 connections. Under conditions of optimal iodine supply of rats, the number of very high direct connections passing through the nodal points was 2, the number of high – 0, the number of salient direct connections – 2, while the number of moderate indirect connections was 6 (Fig. 1).

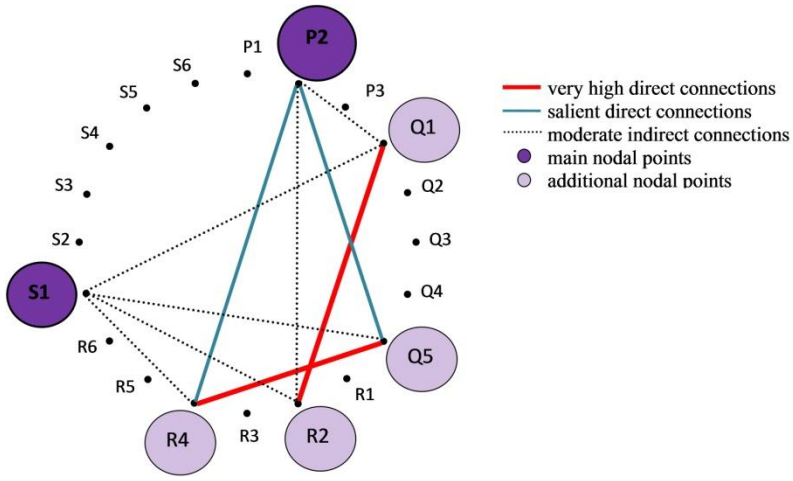

Figure 1: Graphic representation of the nodal points' correlation portrait profile structure of the follicular thyrocytes' transport capability in intact rats (group 1)

The connective filling of the correlation portrait nodal points of the intact rats' follicular thyrocytes transport capability profile is presented in Tab. 2.

Table 2

Structure of the main and additional nodal points of the transport capability profile of follicular thyrocytes in intact rats

Nodal point	Correlations between ultrastructural elements of nodal points with indication of their signs quality	Symbols of nodal points elements	Correlation coefficient (r)
P2*	moderate folding of basal cytoplasmic membranes - no additional inclusions in the pericapillary space	P2—Q5	0.612
P2*	moderate folding of basal cytoplasmic membranes - small pseudopodia of endotheliocytes	P2—R4	0.612
P2*	moderate folding of basal cytoplasmic membranes - unchanged (normal) endotheliocytes	P2—R2	−0.408
P2*	moderate folding of basal cytoplasmic membranes - insignificant width of pericapillary space	P2—Q1	−0.408
S1*	no features (normal) microcapillary bed - insignificant width of pericapillary space	S1—Q1	−0.408
S1*	no features (normal) microcapillary bed - no additional inclusions of pericapillary space	S1—Q5	−0.408

S1*	no features (normal) microcapillary bed - unchanged (normal) endotheliocytes	S1—R2	−0.408
S1*	no features (normal) microcapillary bed - small pseudopodia of endotheliocytes	S1—R4	−0.408
Q5	no additional inclusions of pericapillary space - small pseudopodia of endotheliocytes	Q5—R4	1.000
R2	unchanged (normal) endotheliocytes - insignificant width of pericapillary space	R2—Q1	1.000

Note. The symbol (*) indicates the main nodes

Nodal point P2, through its direct connections (r=0.612) with Q5 and R4, contributes to the harmonization of indirect connections (r=−0.408) with Q1 and R2, which have a certain disharmonious potential. Nodal point S1 harmonizes indirect connections (r=−0.408) traced between Q1, Q5, R2, R4, which can cause instability of the transport system. At the same time, a certain instability of the system, which is indicated by indirect connections S1, may be a sign of its ability to adapt. Under conditions of optimal odine supply to rats, the correct transport of the hormonal product by the microcapillary bed occurs in the presence of 2 main components: the relationship "Q1—R2 (insignificant width of the pericapillary space - normal endotheliocytes)" and "Q5—R4 (no inclusions in the pericapillary space - small pseudopodia of endotheliocytes)", very high direct connections (r=1.000) which provide functional balance in the transport system.

4.2. Studying the features of the nodal points of the correlation portrait of the follicular thyrocytes transport capability profile in the conditions of alimentary iodine deficiency (group 2)

The actual features of the studied portrait were P3, Q1, Q2, Q5, R2, R3, R5, S1, between which very high connections (1.00≥| r |≥ 0.91) – 1 (indirect), high connections were traced (0.90≥| r |≥ 0.71) – 1, salient connections (0.70≥| r |≥ 0.51) – 5 (indirect 4), moderate connections (0.50≥|r |≥ 0.31) – 7 (indirect 4). The main nodal points of the portrait were normal (R2) and hypertrophied endotheliocytes (R3), which had 5 connections each; additional nodal points were a significant fold of the basal cytoplasmic membranes of follicular thyrocytes (P3), an insignificant width of the pericapillary space (Q1), no additional inclusions in the pericapillary space (Q5), small pseudopodia of endotheliocytes (R4), no features (normal) microcapillary bed (S1), which had 3 connections. Under conditions of alimentary iodine deficiency, the following connections passed through the nodal points of the correlation portrait: very high – 1 indirect, high – 1 direct, salient – 5 (indirect 4), moderate – 8 (indirect 5) - see Fig. 2.

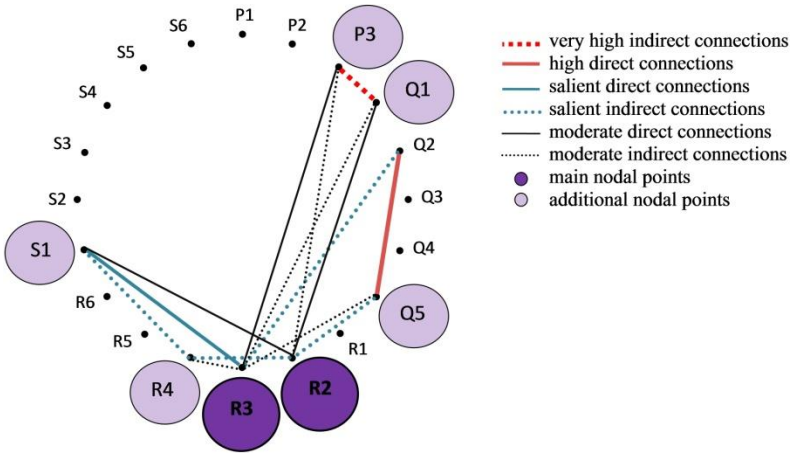

Figure 2: Graphic representation of the nodal points transport capability correlation profile structure of the follicular thyrocytes in the conditions of alimentary iodine deficiency (group 2)

The connective filling of the nodal points of the follicular thyrocytes transport capability correlation portrait profile of rats, which were in conditions of alimentary iodine deficiency, are presented in Tab. 3.

Table 3

Structure of the main and additional nodal points of the transport capability profile of rat follicular thyrocytes in the conditions of alimentary iodine deficiency

Nodal point	Correlations between ultrastructural elements of nodal points with indication of their signs quality	Symbols of nodal points elements	Correlation coefficient (r)
R2*	unchanged (normal) endotheliocytes - no additional inclusions of pericapillary space	R2—Q5	−0.612
R2*	unchanged (normal) endotheliocytes - small pseudopodia of endotheliocytes	R2—R4	−0.612
R2*	unchanged (normal) endotheliocytes - small width of pericapillary space	R2—Q1	0.408
R2*	unchanged (normal) endotheliocytes - no features (normal) microcapillary bed	R2—S1	0.408
R2*	unchanged (normal) endotheliocytes - significant folding of basal cytoplasmic membranes	R2—P3	−0.408
R3*	hypertrophied endotheliocytes - no features (normal) microcapillary bed	R3—S1	0.612
R3*	hypertrophied endotheliocytes - moderate width of pericapillary space	R3—Q2	−0.535
R3*	hypertrophied endotheliocytes - significant folding of basal cytoplasmic membranes	R3—P3	0.408
R3*	hypertrophied endotheliocytes - small width of pericapillary space	R3—Q1	−0.408
R3*	hypertrophied endotheliocytes - no additional inclusions of pericapillary space	R3—Q5	−0.408
R3*	hypertrophied endotheliocytes - small pseudopodia of endotheliocytes	R3—R4	−0.408
P3	significant folding of basal cytoplasmic membranes - insignificant width of pericapillary space	P3—Q1	1.000
Q5	no additional inclusions of pericapillary space - moderate width of pericapillary space	Q5—Q2	0.734
R4	small pseudopodia of endotheliocytes - no features (normal) microcapillary bed	R4—S1	−0.667

Note. The symbol (*) indicates the main nodes

Nodal point R2 through direct communication (r=0.408) R2 with S1 stabilizes indirect connections R2 with R4 (r=−0.612), and with P3 (r=−0.408), which indicate a functional mismatch in the transport of hormonal product by intraorgan microcapillary bed. Another area of the nodal point R2 influence on the activity of thyrocytes is the adaptation of the intraorgan microcapillary bed to the transport of thyroid hormones in conditions of iodine deficiency. Manifestations of this are the following connections: direct with Q1 (r=0.408) and indirect with Q5 (r=−0.612).

The nodal point R3 also has a stabilizing effect on hormone transport. Thus, the direct connection of R3 with S1 (r=0.612) helps to reduce the adverse (unbalancing) effects of indirect connections (r=−0.408) R3 with Q1, Q5, R4 and a direct connection of the same force with P3. Nevertheless, a very high indirect connection between the nodal points P3 and Q1 (r=−1.000) indicates that the system is generally in an unstable state.

4.3. Study of the features of the nodal points correlation portrait of the transport capability profile of follicular thyrocytes when taking 21 μg of organic iodine in conditions of alimentary iodine deficiency (group 3)

The actual features of the studied portrait were P3, Q2, Q3, Q5, R2, R3, R5, S1, between which the following correlations were established (Fig. 3): very high (1.00≥| r |≥0.91) – 3 (of which indirect – 2), salient connections (0.70≥| r |≥0.51) – 11 (6 indirect), moderate connections (0.50≥| r |≥ 0.31) – 7 (of which indirect 5). The main nodal points of the portrait were a significant folding of basal cytoplasmic membranes of follicular thyrocytes (P3), unchanged (normal) endotheliocytes (R2), hypertrophied endotheliocytes (R3), medium (normal) pseudopodia of endotheliocytes (R5), which had 6 connections each. Additional focal points of the portrait were Q2, Q3, S1, which had 5 connections, and Q5, which had 3 connections.

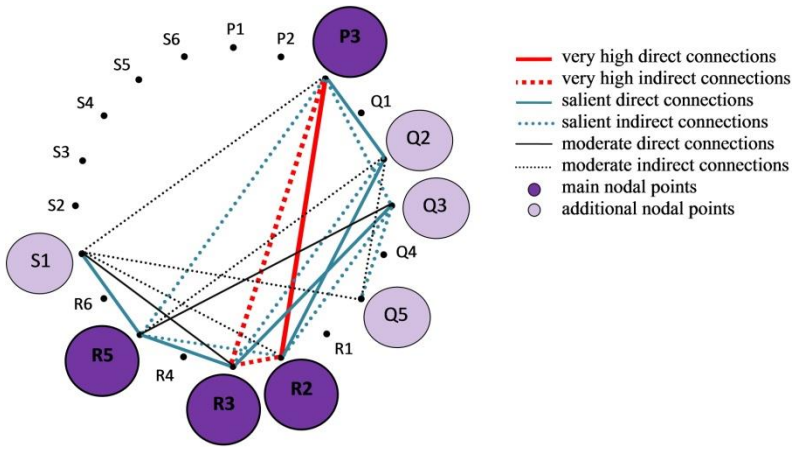

Figure 3: Graphic representation of the nodal points structure of the correlation portrait profile transport capability of follicular thyrocytes when taking the minimum effective dose of organic iodine (21μg/kg body weight) in conditions of alimentary iodine deficiency (group 3)

The connective filling of the nodal points of the transport capability profile correlation portrait of rat follicular thyrocytes, for which the alimentary iodine deficiency was corrected with the minimum effective dose of organic iodine (21μg/kg body weight), is presented in Tab. 4.

Table 4

Structure of the main and additional nodal points of the transport capability profile of rat follicular thyrocytes in the correction of alimentary iodine deficiency by taking the minimum effective dose of organic iodine (21 μg/kg body weight)

Nodal point	Correlations between ultrastructural elements of nodal points with indication of their signs' quality	Symbols of nodal points elements	Correlation coefficient (r)
P3*	significant folding of basal cytoplasmic membranes - unchanged (normal) endotheliocytes	P3—R2	1.000
P3*	significant folding of basal cytoplasmic membranes - hypertrophied endotheliocytes	P3—R3	−1.000
P3*	significant folding of basal cytoplasmic membranes - moderate width of pericapillary space	P3—Q2	0.612
P3*	significant folding of basal cytoplasmic membranes - significant width of pericapillary space	P3—Q3	−0.612
P3*	significant folding of basal cytoplasmic membranes - medium (normal) pseudopodia of endotheliocytes	P3—R5	−0.667
P3*	significant folding of basal cytoplasmic membranes - no features (normal) microcapillary bed	P3—S1	−0.408

R2*	unchanged (normal) endotheliocytes - hypertrophied endotheliocytes	R2—R3	−1.000
R2*	unchanged (normal) endotheliocytes - moderate width of pericapillary space	R2—Q2	0.612
R2*	unchanged (normal) endotheliocytes - significant width of pericapillary space	R2—Q3	−0.612
R2*	unchanged (normal) endotheliocytes - medium (normal) pseudopodia of endotheliocytes	R2—R5	−0.667
R2*	unchanged (normal) endotheliocytes - no features (normal) microcapillary bed	R2—S1	−0.408
R3*	hypertrophied endotheliocytes - significant width of pericapillary space	R3—Q3	0.612
R3*	hypertrophied endotheliocytes - medium (normal) pseudopodia of endotheliocytes	R3—R5	0.667
R3*	hypertrophied endotheliocytes - moderate width of pericapillary space	R3—Q2	−0.612
R3*	hypertrophied endotheliocytes - no features (normal) microcapillary bed	R3—S1	0.408
R5*	medium (normal) pseudopodia of endotheliocytes - no features (normal) microcapillary bed	R5—S1	0.612
R5*	medium (normal) pseudopodia of endotheliocytes - significant width of pericapillary space	R5—Q3	0.408
R5*	medium (normal) pseudopodia of endotheliocytes - moderate width of pericapillary space	R5—Q2	−0.408
Q3	significant width of pericapillary space - no additional inclusions in pericapillary space	Q3—Q5	−0.612
S1	no features (normal) microcapillary bed - no additional inclusions of pericapillary space	S1—Q5	−0.408
Q5	no additional inclusions of pericapillary space - moderate width of pericapillary space	Q5—Q2	−0.408

Note. The symbol (*) indicates the main nodes

Analysis of the correlations in the discussed portrait showed that their combination at the node point P3 improves the transport direction of the thyroid gland. Thus, a very high direct connection of P3 with R2 (r=1.000) and connections of P3 with Q2 (r=0.612) and S1 (r=−0.408) balance the indirect connections of P3 with R3 (r=−1.000), Q3 (r=−0.612) and R5 (r=−0.667), which indicate certain difficulties in transporting the hormonal product.

The connections at the R2 node point indicate an improved transport of thyroid hormones. This is indicated by the direct relationship R2 with Q2 (r=0.612) and the indirect relationship R2 with S1 (r=−0.408) and R5 (r=−0.667). The node point R3 has the same adaptive effect, in which the correlations R3 are connected: direct with Q3 (r=0.612) and R5 (r=0.667), and indirect with S1 (r=−0.408). In turn, the correlations that form the R5 nodal point have a certain stabilizing effect on the transport direction of thyrocytes. These include direct connections R5 with S1 (r=0.612), R3 (r=0.667), Q3 (r=0.408), and indirect connections R5 with R2 (r=−0.667) and P3 (r=−0.667). Peculiarities of correlations in nodal points Q2, Q3, Q5, S1 have already been considered in the study of other nodal points of the discussed correlation portrait.

4.4. Study of the nodal points features of the correlation portrait profile of the follicular thyrocytes transport capability when taking 21 μg of inorganic iodine in conditions of alimentary iodine deficiency (group 4)

The actual characteristics of the correlation portrait were P1, P2, Q2, Q3, Q5, R2, R3, R4, R5, S3, S5, S6, between which the following correlations were established (Fig. 4): very high (1.00≥| r |≥0.91) – 8 (of which indirect - 4), high (0.90≥| r |≥0.71) – 2 (all direct), salient 0.70≥| r |≥0.51) – 25 (17 of them are indirect), moderate 0,50≥| r |≥0,31 – 6 (of which indirect - 1).

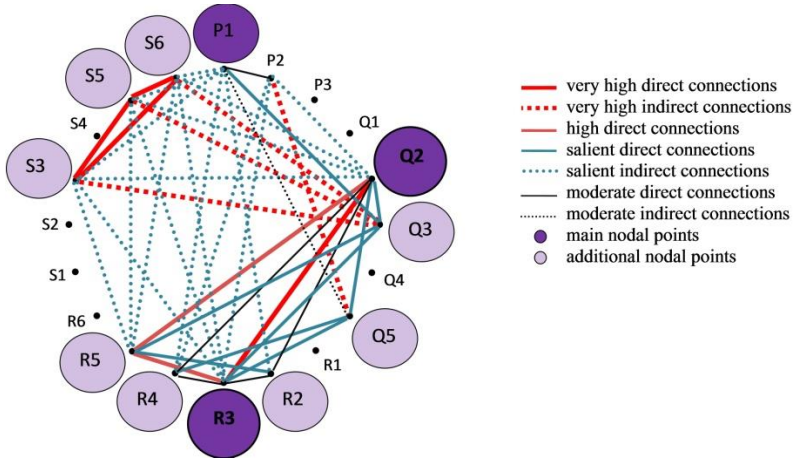

Figure 4: Graphic representation of the nodal points structure of the correlation portrait profile of the follicular thyrocytes transport capability when taking the minimum effective dose of inorganic iodine (21 μg/kg body weight) in conditions of alimentary iodine deficiency (group 4)

The main nodal points of the portrait were a moderate width of pericapillary space (Q2) and hypertrophied endotheliocytes (R3), which had 10 connections each. Additional nodal points of the portrait were P1 – 8 connections; Q3, R5, S3, S5, S6, which had 7 connections each; Q5 and R4 – 5 connections each; R2 – 4 connections. The connection filling of the nodal points correlation portrait of the transport capability profile of rat follicular thyrocytes, for which the alimentary iodine deficiency was corrected with the minimum effective dose of inorganic iodine (21μg/kg body weight), is presented in Tab. 5.

Table 5

Structure of the main and additional nodal points of the transport capability profile of rat follicular thyrocytes in the correction of alimentary iodine deficiency by taking the minimum effective dose of inorganic iodine (21μg/kg body weight)

Nodal point	Correlations between ultrastructural elements of nodal points with indication of their signs' quality	Symbols of nodal points elements	Correlation coefficient (r)
Q2*	moderate width of pericapillary space - hypertrophied endotheliocytes	Q2—R3	1.000
Q2*	moderate width of pericapillary space - medium (normal) pseudopodia of endotheliocytes	Q2—R5	0.791
Q2*	moderate width of pericapillary space - significant width of pericapillary space	Q2—Q3	0.612
Q2*	moderate width of pericapillary space - no additional inclusions in pericapillary space	Q2—Q5	0.612
Q2*	moderate width of pericapillary space - presence of erythrocytes in microcapillary bed	Q2—S3	−0.612
Q2*	moderate width of pericapillary space - presence of mast cells in microcapillary bed	Q2—S5	−0.612
Q2*	moderate width of pericapillary space - presence of fibrin threads in microcapillary bed	Q2—S6	−0.612
Q2*	moderate width of pericapillary space - moderate folding of basal cytoplasmic membranes	Q2—P2	−0.612

Q2*	moderate width of pericapillary space - unchanged (normal) endotheliocytes	Q2—R2	0.408
Q2*	moderate width of pericapillary space - small pseudopodia of endotheliocytes	Q2—R4	0.408
R3*	hypertrophied endotheliocytes - medium (normal) pseudopodia of endotheliocytes	R3—R5	0.791
R3*	hypertrophied endotheliocytes - significant width of pericapillary space	R3—Q3	0.612
R3*	hypertrophied endotheliocytes - no additional inclusions in pericapillary space	R3—Q5	0.612
R3*	hypertrophied endotheliocytes - presence of erythrocytes in microcapillary bed	R3—S3	−0.612
R3*	hypertrophied endotheliocytes - presence of mast cells in microcapillary bed	R3—S5	−0.612
R3*	hypertrophied endotheliocytes - presence of fibrin threads in microcapillary bed	R3—S6	−0.612
R3*	hypertrophied endotheliocytes - moderate folding of basal cytoplasmic membranes	R3—P2	−0.612
R3*	hypertrophied endotheliocytes - unchanged (normal) endotheliocytes	R3—R2	0.408
R3*	hypertrophied endotheliocytes - small pseudopodia of endotheliocytes	R3—R4	0.408
P1	insignificant folding of basal cytoplasmic membranes - significant width of pericapillary space	P1—Q3	0.612
P1	insignificant folding of basal cytoplasmic membranes - unchanged (normal) endotheliocytes	P1—R2	−0.612
P1	insignificant folding of basal cytoplasmic membranes - small pseudopodia of endotheliocytes	P1—R4	−0.612
P1	insignificant folding of basal cytoplasmic membranes - presence of erythrocytes in microcapillary bed	P1—S3	−0.612
P1	insignificant folding of basal cytoplasmic membranes - presence of mast cells in microcapillary bed	P1—S5	−0.612
P1	insignificant folding of basal cytoplasmic membranes - presence of fibrin threads in microcapillary bed	P1—S6	−0.612
P1	insignificant folding of basal cytoplasmic membranes - moderate folding of basal cytoplasmic membranes	P1—P2	0.408
P1	insignificant folding of basal cytoplasmic membranes - no additional inclusions in pericapillary space	P1—Q5	−0.408
Q3	significant width of pericapillary space - presence of erythrocytes in microcapillary bed	Q3—S3	−1.000
Q3	significant width of pericapillary space - presence of mast cells in microcapillary bed	Q3—S5	−1.000
Q3	significant width of pericapillary space - presence of fibrin threads in microcapillary bed	Q3—S6	−1.000
Q3	significant width of pericapillary space - medium (normal) pseudopodia of endotheliocytes	Q3—R5	0.645
R5	medium (normal) pseudopodia of endotheliocytes - unchanged (normal) endotheliocytes	R5—R2	0.645
R5	medium (normal) pseudopodia of endotheliocytes - presence of erythrocytes in microcapillary bed	R5—S3	−0.645

R5	medium (normal) pseudopodia of endotheliocytes - presence of mast cells in microcapillary bed	R5—S5	−0.645
R5	medium (normal) pseudopodia of endotheliocytes - presence of fibrin threads in microcapillary bed	R5—S6	−0.645
S3	presence of erythrocytes in microcapillary bed - presence of mast cells in microcapillary bed	S3—S5	1.000
S3	presence of erythrocytes in microcapillary bed - presence of fibrin threads in microcapillary bed	S3—S6	1.000
S6	presence of fibrin threads in microcapillary bed - presence of mast cells in microcapillary bed	S6—S5	1.000
Q5	no additional inclusions in pericapillary bed - moderate folding of basal cytoplasmic membranes	Q5—P2	−1.000
Q5	no additional inclusions in pericapillary space - small pseudopodia of endotheliocytes	Q5—R4	0.667
R4	small pseudopodia of endotheliocytes - moderate folding of basal cytoplasmic membranes	R4—P2	−0.667

Note. The symbol (*) indicates the main nodes

Correlations that pass through the nodal point Q2 significantly reduce the functional stress caused by iodine deficiency. These include the direct Q2 connections with R3 (r=1.000), R5 (r =0.791), Q3 (r=0.612), (r=0.612), R2 (r=0.408), and R4 (r=0.408). In general, indirect bonds (r=−0.612) Q2 with P2, S3, S5 and S6 indicate difficulties in hormone transport. However, we believe that in combination with other connections that form the discussed node Q2, they are an indication that inorganic iodine improves the transport capability of the intraorgan microcapillary bed.

The nodal point R3 had a similar effect. Thus, the complex of direct connections R3 with R5 (r=0.791), Q3 (r=0.612), Q5 (r=0.612), R2 (r=0.408), R4 (r=0.408) is aimed at stabilizing the functional capability of the microcapillary bed. Indirect connections R3 with S3 (r=−0.612), S5 (r=−0.612), S6 (r=−0.612), and P2 (r=−0.612), which generally indicate a certain inconsistency in the transport of the hormone under iodine deficit, are largely offset by other correlations that pass through the discussed node point.

Node point P1 harmonizes other correlations that pass through it. This is indicated by the complex of indirect connections of P1 with such indices of the state of endotheliocytes and microcapillary bed as R2 (r=−0.612), R4 (r=−0.612), S3 (r=−0.612), S5 (r=−0.612), S6 (r=−0.612), Q5 (r=−0.408). This aspect of the influence of the nodal point is evidenced by the direct connections of P1 with Q3 (r=0.612) and P2 (r=0.408). The nodal point S3, through its ultrastructural element S3, was connected by very high direct correlations (r=1,000) with S5 and S6.

Given the ability of erythrocytes to bind thyroid hormones to their membranes and distribute them to the bloodstream after binding to plasma proteins, we consider these connections to be an adaptive mechanism aimed at improving the transport of the hormonal product. Other connections that passed through the nodal point S3 were indirect connections S3 with P1 (r=−0.612), Q2 (r=−0.612), Q3 (r=−1.000), R3 (r=−0.612), R5 (r=−0.645), which also indicated that one of the means of transporting thyroid hormones by the microcapillary bed was erythrocytes.

Thus, the study of the nodal points connection content of correlation portraits and nomenclatures of these correlations made it possible to better understand the essence of the interactions of ultrastructures of the studied profile and to determine the general direction of their action in different study conditions. Thus, with optimal provision of the body of rats with iodine system-forming nodal points of the follicular thyrocytes transport capability correlation portrait were moderate folding of the basal follicular thyrocytes cytoplasmic membranes (P2) and no features (normal) microcapillary bed (S1), provide both activity and balance in the system of “transportation of the produced hormonal product by the intraorganic microcapillary bed”.

On the other hand, in the conditions of alimentary iodine deficiency, nodal points became especially important, the basis of which is significant folding of basal follicular thyrocytes cytoplasmic membranes (P3), normal endotheliocytes (R2), hypertrophied endotheliocytes (R3) and

medium (normal) pseudopodia of endotheliocytes (R5). Through the connections of these system-forming nodal points, the hormone was transported under adverse conditions of iodine deficiency.

When correcting alimentary iodine deficiency with organic iodine, the transport of thyroid hormones provided stabilizing connections of nodal points, the system-forming basis of which was significant folding of basal cytoplasmic membranes of follicular thyrocytes (P3), unchanged and hypertrophied endotheliocytes (R2 and R3).

At the same time, when taking a similar dose of inorganic iodine, the transport of hormones was provided by a complex system of nodal points with stabilizing complexes of correlations. In this case, the system-forming basis of nodal points was an insignificant folding of the follicular thyrocytes' basal cytoplasmic membranes (P1), moderate width of the pericapillary space (Q2), hypertrophied endotheliocytes (R3) and the presence of erythrocytes in the microcapillary bed (S3).

We noticed that the nodal point S1, the system-forming basis of which no features (normal) microcapillary bed, is a frequent component of correlation portraits of the studied direction of follicular thyrocytes. Because many indirect connections pass through it, we consider it an important stabilizing element of the intraorgan system of thyroid hormone transport. Comparison of the structural organizations of the correlation portraits' nodal points studied in the presented work showed that the closest to the indices of intact rats (norms) were the data of rats that consumed organic iodine. The results are presented in the final Tab. 6.

Table 6

Peculiarities of ligament filling of nodal points of correlation portraits in the transport direction of activity of follicular thyrocytes at various supply of the body with iodine

Experimental conditions (group)	Total number of significant correlations	Number of very high connections	Number of high connections	Number of salient connections	Number of moderate connections
Vivar feed (group 1)	10	2 (all direct)	null	2 (all direct)	6 (all indirect)
Iodine deficiency in the diet (group 2)	14	1 (indirect)	1 (direct)	5 (4 indirect)	7 (4 indirect)
Organic iodine (group 3)	20	2 (1 indirect)	null	11 (6 indirect)	7 (5 indirect)
Inorganic iodine (group 4)	41	8 (4 indirect)	2 (all direct)	25 (18 indirect)	5 (1 indirect)

Thus, the performed study became the basis for a certain revision of our previous views on the correlation portraits' nodal points as exclusively places of accumulation of correlations. Taking into account the obtained data, we believe that the nodal points of the correlation portraits of the transport direction largely indicate changes in the activity of thyrocytes as hormone-producing cells.

5. Conclusions

1. Nodal points of correlation portraits are mathematical resultants of changes in cells. This permits to study the functional dependencies that occur during the activity of hormone-producing cells.

2. The interaction of correlations in the nodal points of correlation portraits has a stabilizing and adaptive effect on the studied activity of the cell, which makes the nodal points important elements of the regulating system.

3. A large number of nodal points in the correlation portrait may be a sign of a certain instability of the whole system.

4. When several correlations of a correlation portrait pass through one nodal point, their mutual potentiation or mutual weakening is possible, and the effect is directly proportional to the number of connections.

5. In the study of the transport direction of follicular thyrocytes, the most informative is the study of the main nodal points of correlation portraits.

6. The presence of additional nodal points in the correlation portraits of the follicular thyrocytes transport direction indicates significant reserve capability of follicular thyrocytes as hormone-producing cells.

7. Analysis of the described nomenclature of the correlation portraits' nodal points showed the variety of activities, stability and adaptation of the hormonal product transportation system in the correction of iodine deficiency with organic and inorganic iodine. This proves that the thyrocyte is a cybernetic self-regulatory system.

6. References

[1] O. Ryabukha, I. Dronyuk, The portraits creating method by correlation analysis of hormone-producing cells data, in: Proceedings of the 1st. International Workshop on Informatics and Data-Driven Medicine, IDDM '18, CEUR-WS.org, Aachen, Germany, 2018, vol. 2255, pp. 135–145. URL: http://ceur-ws.org/Vol-2255/paper13.pdf.

[2] O. Ryabukha, I. Dronyuk, Applying of information technologies for study of the thyroid gland follicular thyrocytes' synthetic activity, in: Proceedings of the 3rd International Conference on Informatics and Data-Driven Medicine, IDDM '20, CEUR-WS.org, Aachen, Germany, 2020, vol. 2753, pp. 323–337. URL: http://ceur-ws.org/Vol-2753/paper23.pdf.

[3] M. J. Caplan, Functional organization of the cell, in: W. F. Boron, E. L. Boulpaep (Eds.), Medical Physiology, 3rd. ed., Elsevier, Philadelphia, 2016, pp. 8–46.

[4] G. G. Avtandilov, Medical morphometry: A guide, Meditsina, Moscow, 1990. [in Russian]

[5] M. Tiwari, A mathematical applications into the cells, Journal of Natural Science, Biology and Medicine 3 (2012) 19–23. doi:10.4103/0976-9668.95937.

[6] O. I. Ryabukha, Substantiation of conceptual apparatus for mathematical studies on the hormone-producing cell activity, Bulletin problems biology and medicine 3, 1 (2018) 234–237. doi:10.29254/2077-4214-2018-3-1-145-234-237. [in Ukrainian]

[7] M. Tighe, C. A. Pollino, S. C. Wilson, Bayesian networks as a screening tool for exposure assessment, Journal of Environmental Management 123 (2013) 68–76. doi:10.1016/j.jenvman.2013.03.018.

[8] L. L. Williams, K. Quave, Regression analysis, in: Quantitative Anthropology: A Work-book, Academic Press, San Diego, CA, 2019, pp. 115–122. doi:10.1016/B978-0-12-812775-9.00009-8.

[9] H. A. Miot, Correlation analysis in clinical and experimental studies, Jornal Vascular Brasileiro 17, 4 (2018) 275–279. doi:10.1590/1677-5449.174118.

[10] M. M. Gupta, Forty-five years of fuzzy sets and fuzzy logic – A tribute to Professor Lotfi A. Zadeh (the father of fuzzy logic), Scientia Iranica 18 (2011) 685–690. doi:10.1016/j.scient.2011.04.023.

[11] U. Dev, A. Sultana, D. Saha, N. Mitra, Application of fuzzy logic in medical data interpretation, Bangladesh Journal of Scientific and Industrial Research 49, 3 (2015) 137–146. doi:10.3329/bjsir.v49i3.22127.

[12] L. A. Zadeh, Can Mathematics Deal with Computational Problems Which Are Stated in a Natural Language? Logic Colloquium, UC Berkeley, 2011. URL: http://philosophy.berkeley.edu/events/detail/793.

[13] O. I. Ryabukha, I. M. Dronyuk, Application of correlation analysis in cytology: Opportunities to study specific activity of follicular thyrocytes, Regul. Mech. Biosyst. 3 (2019) 345–351. doi:10.15421/021953.

[14] E. J. Barrett, The thyroid gland, in: W. F. Boron, E. L. Boulpaep (Eds.), Medical Physiology, 3rd. ed., Elsevier, Philadelphia, 2016, pp. 1006–1017.

[15] P. N. Taylor, D. Albrecht, A. Scholz, G. Gutierrez-Buey, J. H. Lazarus, C. M. Dayan, O. E. Okosieme, Global epidemiology of hyperthyroidism and hypothyroidism, Nat. Rev. Endocrinol. 15, 5 (2018) 301–316. doi:10.1038/nrendo.2018.18.

[16] M. A. Shelamova, N. I. Insarova, V. G. Leshchenko, Basis of statistical analysis of biomedical data using Excel: study guide. Belarusian State Medical University, Minsk, 2017. [in Russian]

[17] E. V. Plashchevaya, V. A. Smirnov, N. V. Nigei, V. A. Lysak, Probabilistic method of diagnosis in medicine. The main types of medical logic, in: Study Guide for Practical Training in Medical Informatics, Amur State Medical Academy, Blagoveshchensk, 2014, p. 176. [in Russian]
[18] H. Akoglu, User's guide to correlation coefficients, Turkish Journal of Emergency Medicine 18, 3 (2018) 91–93. doi:10.1016/j.tjem.2018.08.001.
[19] P. Schober, C. Boer, L. A. Schwarte, Correlation Coefficients: Appropriate Use and Interpretation, Anesthesia & Analgesia 126, 5 (2018) 1763–1768. doi:10.1213/ANE.0000000000002864.
[20] O. Riabukha, Application of new information technologies for the study of cell activity, in: Proceedings of the 11th. International Conference on Perspective Technologies and Methods in MEMS Design, MEMSTECH '15, IEEE, New York, NY, 2015, vol. 1, pp. 69–71. URL: https://ieeexplore.ieee.org/xpl/conhome/7297752/proceeding.
[21] N. M. Ali Rajab, M. Ukropina, M. Cakic-Milosevic, Histological and ultrastructural alterations of rat thyroid gland after short-term treatment with high doses of thyroid hormones, Saudi Journal of Biological Sciences 24, 6 (2017) 1117–1125. doi:10.1016/j.sjbs.2015.05.006.